

höchste untersuchte Anthracenkonzentration ist die Abklingdauer im ganzen Temperaturbereich praktisch konstant. Das Phasenwinkeldiagramm (als Beispiel Abb. 9) für die Anthracenemission bei direkter und indirekter Anregung zeigt zwar eine deutliche Verlängerung des Phasenwinkels bei indirekter Anregung, aber keine volle Additivität der Phasenwinkel von Grundgitter- und Gastfluoreszenz. Die Aufklärung aller dieser Unregelmäßigkeiten erfordert weitere Untersuchungen.

Die direkt angeregte Anthracenabklingdauer fällt zu höheren Temperaturen hin ab. Dies läßt sich auch hier als thermische Löschung interpretieren, wie die Darstellung eines Beispiels in Abb. 10 zeigt.

Aus Neigung und Achsenabschnitt ergeben sich für die Aktivierungsenergie und den Frequenzfaktor die Werte

$$\Delta E = (0,06 \pm 0,005) \text{ eV},$$

$$s^* = (7,4 \pm 1,0) \cdot 10^8 \text{ s}^{-1}.$$

Die Arbeit wurde im I. Physikalischen Institut der Justus Liebig-Universität Gießen mit finanzieller Unterstützung durch die Deutsche Forschungsgemeinschaft durchgeführt. Herrn Professor Dr. A. SCHMILLEN danke ich für zahlreiche anregende Diskussionen und Ratschläge und Herrn Professor Dr. W. HANLE für sein förderndes Interesse an der Arbeit. Mein besonderer Dank gilt auch Herrn Dr. BELITZ für seine kollegiale Mithilfe bei der Kristallpräparation.

Nonisothermal Diffusion Measurements on Granular Solids: Noble Gas Diffusion in Fused Silica

M. ABE *, B. RAUCH **, and W. W. BRANDT

Chemistry Department and Laboratory for Surface Studies, University of Wisconsin-Milwaukee, Milwaukee, Wisconsin, USA

(Z. Naturforsch. 26 a, 997—1004 [1971]; received 26 February 1971)

Samples of fused SiO_2 and of a soda-lime glass were exposed to He, Ne, and Ar at temperatures between 523 and 763 °K, cooled to room temperature, transferred to a desorption cell, and then heated slowly and uniformly. The cell was connected to a mass spectrometer and the desorption rates were measured as a function of time. From the data, the parameters E and D_0 of the Arrhenius equation for the diffusion coefficient [$D = D_0 \exp(-E/RT)$] were calculated.

The results were found to agree rather well with literature data obtained on similar glasses using isothermal methods. Since the nonisothermal technique may be very useful for the study of granular materials and powders, the problems related to the presence of a grain size distribution and to the irregularities of grain shapes are treated in this study in some detail.

Introduction

The analysis and systematic description of granular materials has received much attention in recent years¹⁻³, yet up to now there have been only very few attempts to evaluate diffusion data obtained on powder samples in a fairly thorough way, for example, taking into account the grain size distribu-

tion which is usually present. PILCHOWSKI and his coworkers⁴⁻⁶ discussed the careful evaluation of sorption or desorption data, and outlined a computational method to cope with this specific problem. LAGERWALL and SCHMELING⁷ discussed the probable consequences of having a grain size distribution in samples they used in post-irradiation diffusion studies. Neither group of workers tested their

Reprints request to Prof. Dr. W. W. BRANDT, Department of Chemistry, University of Wisconsin-Milwaukee, Milwaukee, Wisc. 53 201, USA.

* Present address: Department of Chemistry, Tokyo Institute of Technology, Tokyo, Japan.

** Present address: Institut für Physikalische Chemie, Gutenberg-Universität, Mainz, Germany.

¹ T. ALLEN, Particle Size Measurement, Chapman and Hall, Ltd., London 1968.

² R. R. IRANI and C. F. CALLIS, Particle Size: Measurement, Interpretation, and Application, John Wiley & Sons, Inc., New York 1963.

³ Particle Size Analysis, Proceedings of a Conference organized by the Society for Analytical Chemistry, published by the same society, London 1966 (editor's name not given).

⁴ K. PILCHOWSKI, F. DAVES, and F. WOLF, Koll.-Z.—Z. Pol. 225, 6 [1968].

⁵ K. PILCHOWSKI, F. DAVES, and F. WOLF, Koll.-Z.—Z. Pol. 230, 328 [1969].

⁶ F. DAVES, K. PILCHOWSKI, and F. WOLF, Ber. Bunsenges. Phys. Chemie 73, 99 [1969].

⁷ T. LAGERWALL and P. SCHMELING, European Atomic Energy Community-Euratom, Report No. EUR 595.e, Presses Academiques Européennes, 98 Chaussée de Charleroi, Brussels, 6, Belgium, 1964.



Dieses Werk wurde im Jahr 2013 vom Verlag Zeitschrift für Naturforschung in Zusammenarbeit mit der Max-Planck-Gesellschaft zur Förderung der Wissenschaften e.V. digitalisiert und unter folgender Lizenz veröffentlicht: Creative Commons Namensnennung-Keine Bearbeitung 3.0 Deutschland Lizenz.

Zum 01.01.2015 ist eine Anpassung der Lizenzbedingungen (Entfall der Creative Commons Lizenzbedingung „Keine Bearbeitung“) beabsichtigt, um eine Nachnutzung auch im Rahmen zukünftiger wissenschaftlicher Nutzungsformen zu ermöglichen.

This work has been digitalized and published in 2013 by Verlag Zeitschrift für Naturforschung in cooperation with the Max Planck Society for the Advancement of Science under a Creative Commons Attribution-NoDerivs 3.0 Germany License.

On 01.01.2015 it is planned to change the License Conditions (the removal of the Creative Commons License condition "no derivative works"). This is to allow reuse in the area of future scientific usage.

ideas in any detail using actual experimental results. GALLAGHER⁸ studied the diffusion controlled oxidation of UO_2 and $\text{PrO}_{1.5}$ and was able to fit his rate data by computed curves corresponding to reasonable size distributions, but he did not measure the distributions of the actual samples he used.

For several reasons which will be discussed later, a number of nonisothermal desorption experiments have been carried out in this laboratory^{9,10}, and idealized desorption rate curves (or desorption transients) have been computed to facilitate the evaluation of the experimental results. It now appears that the nonisothermal method is particularly useful if one wishes to account for the presence of a size distribution in a granular sample. This will be discussed in some detail in the present paper; actual desorption transient data will be analyzed using experimental and assumed size distributions.

A second common source of systematic errors encountered in sorption or desorption studies lies in the irregularity of particle shapes; the systematic treatment of this three-dimensional problem is known to be difficult¹¹, but experimental comparisons permit one to estimate how serious this effect may be and to correct for it in an approximate way. In the approach proposed here, the size distribution and shape corrections are interrelated, as will be discussed below.

As a second goal of the present study, the results from the nonisothermal technique will be compared to those obtained by more conventional methods. It seemed appropriate to measure the diffusion coefficients of noble gases in fused silica, since there are several earlier literature reports on the diffusion of noble gases in this glass¹²⁻¹⁶.

Review of Isothermal and Nonisothermal Methods

A solid sorbent consisting of one or many homogeneous spheres of uniform diameter, $2a$, and diffusion coefficient, D , will under isothermal condi-

tions sorb or desorb an amount of sorbate, M_t , which is given as a function of time, t , by

$$M_t = M_\infty \left(1 - \frac{6}{\pi^2} \sum_{m=1}^{\infty} \frac{1}{m^2} \exp(-m^2 \pi^2 D t/a^2) \right). \quad (1)$$

D is assumed to be independent of concentration, if Eq. (1) is to hold, and the concentration of sorbate in the gas phase is to change as a step function at time $t=0$, and to remain constant thereafter, while it is assumed to be uniform within the sorbent, at $t=0$. M_∞ is the total amount sorbed or desorbed after very long (infinite) time¹⁷.

Mass spectrometric desorption studies require that the sorbate released during the experiment be pumped off continuously. The quantity measured, R^* , is thus proportional to the time derivative of M_t , or R , that is

$$R \equiv \frac{dM_t}{dt} = 6 M_\infty \frac{D}{a^2} \sum_{m=1}^{\infty} \exp(-m^2 \pi^2 D t/a^2). \quad (2)$$

If the experimental data are plotted as $\log R^*$ against $\log t$, and Eq. (2) as $\log R$ against $\log \tau$, where $\tau \equiv D t/a^2$, one can superpose the two plots and determine pairs of corresponding τ and t values, provided of course that the experimental and computed curves are of similar shape. D can then readily be calculated from the τ , t pair so obtained, since $D = (\tau/t) a^2$. The radius, a , is determined separately.

The evaluation of nonisothermal desorption experiments requires that one knows, or assumes, the way D depends on the temperature. Frequently the Arrhenius equation for the diffusion coefficient is valid within experimental errors;

$$D = D_0 \exp(-E/RT) \quad (3)$$

here D_0 is the pre-exponential factor, E the activation energy, R the gas constant, and T the absolute temperature. Once the temperature program for a given desorption experiment is specified, for example, if

$$T = T_0 + \beta t \quad (4)$$

⁸ K. J. GALLAGHER, in: Proceedings of the 5th International Symposium on the Reactivity of Solids, Munich 1964; Elsevier Publ. Co., Amsterdam 1969, p. 192.

⁹ W. W. BRANDT, Int. J. Heat Mass Transfer **13**, 1559 [1970]

¹⁰ W. W. BRANDT, American Society for Information Sciences, # NAPS-00939, 1970.

¹¹ H. H. HAUSNER, Ref. ³, p. 20.

¹² D. E. SWETS, R. W. LEE, and R. C. FRANK, J. Chem. Phys. **34**, 17 [1961].

¹³ R. C. FRANK, D. E. SWETS, and R. W. LEE, J. Chem. Phys. **35**, 1451 [1961].

¹⁴ K. P. SRIVASTAVA and G. J. ROBERTS, Phys. Chem. Glasses **11**, 21 [1970].

¹⁵ G. A. WILLIAMS and J. B. FERGUSON, J. Amer. Chem. Soc. **46**, 635 [1924].

¹⁶ R. M. BARRER, Diffusion in and through Solids, University Press, Cambridge (Mass.) 1951, p. 141.

¹⁷ J. CRANK, The Mathematics of Diffusion, Clarendon Press, Oxford 1957, p. 86, Eq. (6.20).

where T_0 is the starting temperature and β is the heating rate, then one can express D as a function of t and define a quantity¹⁸ τ_n ,

$$\tau_n = \frac{1}{a^2} \int_0^t D(t') dt' \quad (5)$$

using τ_n instead of Dt/a^2 in Eq. (1) yields $M_{t,n}$ the amount of gas sorbed or desorbed under nonisothermal conditions, as a function of τ_n , subject to Eqs. (3) and (4):

$$M_{t,n}(t) = M_\infty \left(1 - \frac{6}{\pi^2} \sum_{m=1}^{\infty} \frac{1}{m^2} \exp(-m^2 \pi^2 \tau_n) \right). \quad (6)$$

The time derivative of $M_{t,n}$, that is $R_n \equiv dM_{t,n}/dt$, is proportional to the measured sorbate signal heights, R_n^* , analogous to the isothermal case. R_n can be considered a function of E and $(D_0/a^2 \beta)$, and instead of attempting a graphical superposition of the experimental and theoretical or computed bell-shaped transient curves, it is often more convenient to characterize each experimental curve by the temperature where the maximum occurs, $T_{\max, \exp}$, and by its half-width, ΔT_{\exp} . Using previously computed transient curves together with $T_{\max, \exp}$ and ΔT_{\exp} values, one can get first estimates of E and $(D_0/a^2 \beta)$, as described in some detail earlier⁹.

The precision and accuracy of isothermal and nonisothermal techniques will be discussed below, after the presentation of the experimental results.

Experimental

Sample Origin and Preparation

The samples of fused SiO_2 used were of high purity grade, General Electric Type 151, and Amersil commercial grade; the soda-lime glass consisted of small spheres, of nominal diameter, 300μ , Lapine Catalog No. 183-35. GeO_2 was Alfa Inorganics Ventron grade of high purity, remelted and characterized in some detail as described in a subsequent publication¹⁹. The SiO_2 and GeO_2 samples were ground and sieved, using woven mesh sieves for large size fractions and an acoustic device, "Sonic Sifter", Allen-Bradley Model L 3, with a set of electroformed sieves for the separation of small grain size fractions. The relative humidity during storage, grinding, and sieving was low, especially when handling the somewhat moisture sensitive GeO_2 . Completely dry conditions were not produced during the sieving process so as to avoid serious electrostatic problems. A typical size distribution obtained

in this way is presented in Table 1. The diameters listed were measured microscopically, in random directions across the irregular grains, the particles being selected at random from the overall sample. The sizes so measured are equivalent to the edge lengths of rect-

Table 1. Typical grain size distribution (Sample C of Table 2).

Diameter (rel. units)	Number of Grains (%)
0-1	0
1-2	1
2-3	5
3-4	1
4-5	7
5-6	24
6-7	27
7-8	17
8-9	11
9-10	5
10-11	2
above 11	0

angles circumscribing the irregular two-dimensional projections at random orientations, without attempting to characterize the particle shapes in some systematic way²⁰. The number average diameters determined by this method and the approximate half-widths of the size distributions for the various samples are summarized in Table 2. It is important to note that the "size distribution" discussed here is a composite measure of the grain size distribution as such and of the shape irregularity.

Table 2. Sample characteristics; fused silica and soda-lime glass samples.

Sample	Material	Origin	Number Average Grain Diameter ^a	Relative Variance ^b
A	SiO_2	Amersil Commercial Grade	88μ	.086
B	SiO_2	Amersil Commercial Grade	132μ	.113
C	SiO_2	G. E. Type 151	120μ	.086
D	SiO_2	G. E. Type 151	1.22 cm	.044
E	SiO_2	G. E. Type 151	4.23μ	.329
F	SiO_2	G. E. Type 151	0.91 cm	.0033
G	SiO_2	G. E. Type 151	208μ	.044
H	Soda-lime Glass		117μ	.125

^a By microscopic analysis, see text.

^b Relative variance = $\frac{1}{(\bar{d})^2} \left(\overline{d^2} - (\bar{d})^2 \right) = \frac{\overline{d^2}}{(\bar{d})^2} - 1$,
where d is the grain diameter.

¹⁸ See Ref. 17, pp. 147, Eq. (9.3).

¹⁹ W. W. BRANDT and B. RAUCH, to be published.

²⁰ See Ref. 11, Fig. 2.

Sorption of Noble Gases

In preparation for isothermal or nonisothermal desorption measurements, the samples were heated to a medium or high temperature, degassed, and exposed to the sorbate gas, usually over night and at pressures between 0.5 and 1.0 atm. The sorption temperature was chosen such that the samples would be saturated, at the gas pressure used, judging from some desorption data obtained in exploratory experiments.

Isothermal Desorption Experiments

The saturated samples were cooled while still exposed to the sorbate gas, and transferred under a blanket of dry nitrogen to another vessel which could be connected to a medium resolution mass spectrometer, Hitachi-Perkin-Elmer Model RMU-6E with a resolution of $M/\Delta M \geq 1800$, based on the 10% valley definition. The measurement of the desorbing gas concentrations was started as soon as the pressure in the system had reached the operating range of the spectrometer from above ($< 10^{-5}$ mm Hg), that is, usually after 4 to 9 min. In one version of the experimental apparatus it was possible to transfer the sample in vacuum within a few seconds without cooling it first, such that the first desorption rates could be measured

even sooner, that is, about 3 min after the transfer. An automatic timer was used to control the mass spectrometer over long periods of time, as described earlier²¹. Standard leaks, Hastings-Rayquist OG-Series, were connected to the system in the vicinity of the sample cell and the corresponding mass signals were monitored together with the sorbate peak of interest. In this way, the impact of systematic errors due to minor fluctuations in spectrometer sensitivity and in system pressure was minimized.

Nonisothermal Desorption Experiments

The saturated and cooled samples were transferred to the desorption vessel, as described previously, and they were subsequently again degassed for a short period of time. Finally the sample temperature was increased at a uniform rate, somewhere between 2.7 and 4.7 ($^{\circ}\text{K}/\text{min}$). The mass spectrometric measurements as such were carried out as described above.

Experimental Results

The principal results from the nonisothermal desorption studies on fused SiO_2 and on the soda-lime glass beads are shown in Table 3. The Ar results are

Table 3. Summary of principal results, sorption times and temperatures, $T_{\text{max, exp}}$ and ΔT_{exp} , and Arrhenius Parameters E and $\log D_0$.

Run ^a Number	Gas	Sample ^b	Sorption Time (hrs)	Sorption Temp. ($^{\circ}\text{K}$)	$T_{\text{max, exp}}$ ($^{\circ}\text{K}$)	ΔT_{exp} ($^{\circ}\text{K}$)	E^c (kcal/mole)	Log D_0^c
50/1	He	D	4	751	627.6	440.7	(6.5) 6.7	(.14—3) .17—3
63/1	He	F	18	717	580.6	342.7	(7.1) 7.1	(.44—3) .44—3
65/1	He	F	16	751	564.5	362.7	(6.4) 6.4	(.19—3) .19—3
19/1	Ne	A	15	759	440.4	134.0	(10.4) 10.9	(.22—4) .40—4
19/2	Ne	B	17	757	455.0	149.3	(9.9) 10.7	(.33—4) .60—4
20/1	Ne	B	17	749	452.8	151.9	(9.7) 10.2	(.24—4) .39—4
49/1	Ne	C	16	749	453.1	127.5	(11.5) 12.1	(.13—3) .34—3
61/1	Ne	G	18	746	486.8	151.0	(11.2) 11.6	(.01—3) .11—3
59/2	Ar	E	17	743	794.4	249.1	(18.1) 22.8	(.32—7) .36—6
62/1	Ar	E	14	763	791.6	257.0	(17.6) 21.9	(.16—7) .14—6
55/1	Ne	H	12	523	595.0	185.0	(13.7) 14.4	(.41—4) .59—4

^a The run numbers indicate the chronological order of the experiments except for 55/1, which was done first.

^b For sample grain size distributions, see Table 2.

^c Values in parentheses are uncorrected; others are corrected for presence of distributions (see text).

included to demonstrate the range of usefulness of the nonisothermal method; there seem to be no literature values available for comparison.

The errors in the data presented here fall into several categories; the probable effect of systematic temperature errors and of pressure transients will be discussed at this point, while the effects of the grain size distribution present, of particle shape irregularities, and of the random errors in the temperature will be estimated at a later point.

Isothermal desorption studies usually require that the sample be heated to the desired temperature of desorption as quickly as is possible. The measured rates of desorption are of course too low, as long as temperature equilibrium has not been reached, and the desorption rate curves, therefore, tend to show a fictitious maximum at short times, that is 3 to 9 min after the start, in the present study. This effect is easily recognized but it cannot be readily eliminated completely. Even more insidious errors are likely to arise if atmospheric or blanket gases are picked up during the transfer operation either by the sample, the interior walls of the desorption vessel, or by the vacuum grease in joints and stop-cocks, and if such gases are released during the desorption measurements. The ratio of mass signals, such as the sorbate signal of interest divided by the reference signal coming from a standard leak, may

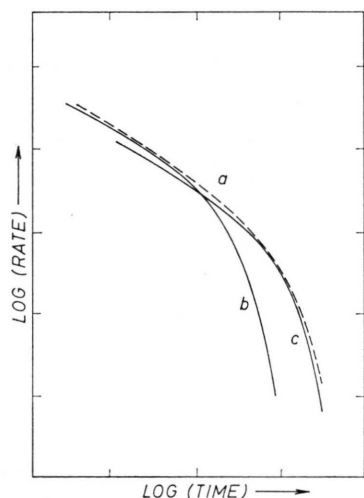


Fig. 1. Isothermal Desorption Rate Curves plotted as $\log(\text{rate})$ against $\log(\text{time})$. The ordinate and abscissa units correspond to unit differences in both logarithms. (a) Experimental curve, with moderate positive deviations of the first portion, due to a pressure transient in the system (see text); (b) and (c) Computed Curves, using Eq. (1), showing the major ambiguity in curve fit resulting from the distortion of Curve (a).

well depend noticeably on the steady state pressures and fluxes throughout the system, presumably due to the differences in pumping speeds for different species. In the present study, this effect tended to raise the early part of a desorption rate curve, as shown in Curve (a) of Fig. 1, and thus it would lead to a major uncertainty in fitting the computed master curve corresponding to Eq. (2) to the data [see Curves (b) and (c) of Fig. 1].

The nonisothermal method has definite advantages as far as these systematic temperature deviations and pressure transient effects are concerned. The sample temperature will normally lag behind the furnace temperature, but if sample and furnace geometry are kept constant the effect can be determined and corrected for; also, this time lag changes only slightly with increasing temperature and thus it does not distort the linearity of the temperature program [see Eq. (4)]. Pressure transients which are related to final degassing of the sample or of the desorption apparatus just prior to the desorption run also are of little concern when using the nonisothermal method, since most of the pressure transient has disappeared when the crucial part of the desorption rate curve is reached near $T_{\text{max, exp}}$. Also, the left and right branches of this rate curve are affected in nearly the same way, as illustrated in Fig. 2, leading to a further reduction of the possible systematic error.

The variations in Ar background usually affect the mass spectrometric measurement of Ar desorp-

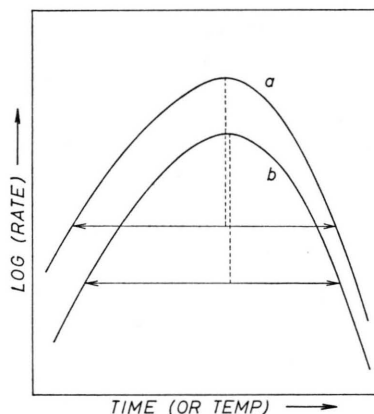


Fig. 2. Nonisothermal Desorption Transients. (a) Experimental curve, with moderate positive errors due to a slow change in system pressure; (b) Computed curve, using Eqs. (3) and (4), etc., showing the fairly minor effect of the pressure problem on the measured half-width, ΔT_{exp} (-----) and the temperature where the maximum occurs, $T_{\text{max, exp}}$ (see text).

The vertical dotted lines are of length $\log 2 = 0.302$.

tion rates since this effect is qualitatively similar to the pressure transients discussed here; it is likewise far less detrimental to nonisothermal rate measurements than to isothermal ones.

As an even more important advantage of the nonisothermal method, it appears that the final results obtained can be readily corrected for the presence of a grain size distribution, as will be described below, while the desorption curves from isothermal experiments cannot easily be corrected to account for this effect since the resulting distortions are qualitatively similar to the distortions arising from the pressure transients [Curve (a), Fig. 1], and cannot be easily separated from the latter.

Computed Results

Computer Program

To assess the effect of the grain size distributions on the Arrhenius parameters E and D_0 [see Eq. (3)] in some detail, a computer program was written to fit the experimental desorption transients by successive approximations.

The essential input parameters needed for the computation were (1) the size distribution histogram, $H(I)$, where I are the measured grain diameters in suitable units, (2) the first estimates of the parameters E and $(D_0/a^2\beta)$ obtained as described above, (3) $T_{\max, \exp}$ and ΔT_{\exp} as defined above, and (4) an approximate value for the heating rate, β [see Eq. (4)]. An average grain radius, a , was computed from $H(I)$, and was used together with β to obtain a first estimate of D_0 from the input $(D_0/a^2\beta)$; errors in " a " and " β " were of no consequence to the process of successive approximations since the final output consisted of an improved estimate of $(D_0/a^2\beta)$, and of E .

The computation first produced τ_n and $M_{t,n}$ values for each fraction, and for many closely spaced temperatures (or times), using Eqs. (5) and (6). The $M_{t,n}$ values were then multiplied by the relative weight of the size fraction considered, summed over all fractions, and used to form difference quotients of $M_{t,n}$ with respect to time, i. e., close approximations to the theoretical desorption rates R_n . From the R_n curves, T_{\max} and ΔT values were computed, compared with the corresponding experimental quantities, $T_{\max, \exp}$ and ΔT_{\exp} , and the discrepancies were used to obtain improved estimates for the

E and D_0 values. The procedure was repeated until the computed T_{\max} and ΔT agreed very closely with $T_{\max, \exp}$ and ΔT_{\exp} .

Effect of Grain Size Distribution and Shape Irregularities

The uncorrected and size distribution-corrected values for E and D_0 are listed in Table 3. It turns out that the correction is always positive, as one would expect, and correlates fairly well but not perfectly with the relative variances of the distributions, as listed in Table 2.

Some of the $T_{\max, \exp}$ and ΔT_{\exp} data obtained were used in conjunction with simple assumed size distributions to compute corrections for the representative E and $(D_0/a^2\beta)$ parameters (Table 4).

Table 4. Computed corrections for parameters E and $\log(D_0/a^2\beta)$ (or $\log D_0$) for normal and log-normal grain size distributions as a function of the variance.

Relative Variance	ΔE	$\Delta[\log(D_0/a^2\beta)]$
Normal Distribution		
0.0029	0.03	0.01
0.0095	0.11	0.03
0.0346	0.30	0.11
0.0759	0.55	0.21
0.1430	0.80	0.32
Log-Normal Distribution		
0.0085	0.10	0.03
0.021	0.20	0.07
0.047	0.40	0.15
0.076	0.67	0.25
0.154	1.09	0.45
0.077 ^b	0.71	0.25

^a The relative variance is calculated as shown in Table 2.

^b The $T_{\max, \exp}$ and ΔT_{\exp} values used are those of Run 61/1; in all other cases those of Run 19/1 were used (see Table 3).

The corrections required are fairly insensitive to the shape of the distributions used (normal and logarithmic-normal) and they depend almost linearly on the relative variance. The results given in Table 4 can be used to estimate corrections for E and $(D_0/a^2\beta)$ values whenever the corrections are not too large.

As mentioned earlier, the distributions determined in this work actually contain an appreciable component arising from the grain shape irregularity. In some cases, that is, for Samples (D) and (F) of Tables 2 and 3, this effect is clearly seen since these samples consisted of single large grains. Equation (6) used in the computation is of course only ap-

proximate for samples of non-spherical shape, and the approach used here is therefore tentative and exploratory. The resulting "corrections" are at least qualitatively correct, as one can see from the solutions to the diffusion equation for spherical and cubic sorbent grains reported by LAGERWALL and ZIMEN^{6, 22}.

A more thorough solution of the shape problem as it enters the size distribution problem most probably depends on future theoretical work¹¹ and the further development of instrumental particle distribution and shape analyzers²³.

Other Errors

Using the computer program, random errors in the temperature also can be easily assessed here. It turns out that small errors in $T_{\max, \exp}$ have little effect on E and D_0 , but ΔT_{\exp} must be obtained with rather high precision. Probably random errors in ΔT_{\exp} and in $H(I)$ are most serious when using the nonisothermal technique as developed up to this time.

Discussion

The E and D_0 parameters resulting from nonisothermal desorption measurements are similar to those obtained by isothermal methods (see Tables 3 and 5) in those cases where comparisons are possible. The sample to sample variation is most likely due to differences in the sample thermal history¹⁴ and perhaps to minor differences in composition. On the whole, the E values from the nonisothermal method are within the range of existing literature data while the D_0 values are possibly somewhat higher (see Table 5). Tentatively, we suggest two possible reasons for this:

(1) The isothermal results are not corrected for the presence of a grain size distribution, or shape irregularities. As discussed earlier, this correction does not appear feasible at the present.

(2) The solubilities of noble gases in fused SiO_2 are known to decrease with increasing temperature²⁴, but conceivably some of the gas sorbed at elevated temperatures is trapped, i. e., it is not de-

Table 5. Comparison of E and D_0 values from nonisothermal and isothermal measurements.

Gas	Sample	E	$\log D_0$	Ref.
He	SiO_2 , G.E. 151	6.7	.27—3	This study
He	SiO_2	5.58 to 6.61	(.483—4) to (.896—4)	12
He	SiO_2	6.3 to 6.61	(.64—4) to (.88—4)	14
He	SiO_2	5.6	(.72—2) to (.08—1) at 293°K (.40—5) to (.31—4) at 773°K	16
Ne	SiO_2 , Amersil	10.6	.56—4	This study
Ne	SiO_2 , G.E. 151	11.9	.23—3	This study
Ne	SiO_2	11.37	.344—4 ^a	13
Ne	SiO_2	9 to 12.0	(.75—5) to (.41—4)	14
Ne	GeO_2	13.7	.5—3	19 nonisothermal
Ne	GeO_2	13.2	.4—4	19 isothermal

^a Value for ^{20}Ne isotope, since the mass signal of that isotope was utilized in the present study.

sorbed at intermediate or low temperatures²⁵. If this effect is appreciable, the left or ascending branch of the experimental desorption transient curves would tend to be too low, and the right or descending branch too high, i. e., $T_{\max, \exp}$ would tend to be too high and ΔT_{\exp} lower than it should be. As a result, the $(D_0/a^2 \beta)$ values determined could be distinctly too high, and the E values slightly increased.

Many additional experimental comparisons are needed to determine whether these effects are important.

One important reason for developing the nonisothermal method lies in that many new systems can probably be studied with it; in some instances, the background uncertainties are far less serious when using this method, compared to the isothermal desorption experiment, as has been the case with the Ar experiments on fused SiO_2 . In other experiments

²² T. LAGERWALL and K. E. ZIMEN, Euratom Report, EUR 1372 e, see Ref. 7.

²³ See Ref. 3, pp 56—153, Sessions (3) and (4).

²⁴ P. L. STUDDT, J. F. SHACKELFORD, and R. M. FULRATH, J. Appl. Phys. **41**, 2777 [1970].

²⁵ A. E. MUSSETT, Geophys. J. Royal Astron. Soc. London **18**, 257 [1969], especially p. 281.

involving vitreous¹⁹ GeO₂, the principal advantage of the method lies in that the devitrification of this glass can be kept low far better when using this relatively rapid technique. Nonisothermal studies on B₂O₃ finally offer the advantage that the pressure gradients arising from the desorption of traces of water usually present in this material can be rendered harmless, as discussed elsewhere²⁶.

Thus far desorption studies involving Kr as sorbate on fused SiO₂ have not been entirely successful, but seem to be feasible*.

In the present report the emphasis has been on the development of the nonisothermal method, but the possible significance of the principal data obtained (Table 3) should be discussed at least very briefly. The increase of E with sorbate molecular size is perhaps to be expected, intuitively. The decrease of D_0 in going from He to Ne and to Ar as sorbate species is in agreement with the recent results of SRIVASTAVA and ROBERTS¹⁴ and the earlier work of SWETS, LEE, and FRANK^{12,13}, if one assumes that the samples used by these latter workers in both studies were identical. Srivastava and Roberts attempted to interpret their results in terms of

known simple molecular models, but with limited success. Specifically, the simple version of the transition state theory used does not take into account that the diffusion paths through a glass may well be related to interstices or gaps with a variety of critical internal dimensions and shapes, rather than a single or average "bottleneck" configuration. The distribution assumed here is of course consistent with the classical model of the random network structure^{12,27}. Clearly at present there are no simple or direct methods for characterizing this distribution. It is possible that diffusion rates, especially when discussed in connection with experimental solubility data, will give some insight into this problem.

Acknowledgment

The work was supported by the U.S. Atomic Energy Commission under Contract AT-(11-1)-1550, and computer funds were furnished by the Laboratory for Surface Studies under a NSF/Departmental Science Development Grant. The authors are indebted to Mr. and Mrs. JOHN WAGNER for many careful determinations of grain size distributions and of surface areas, and to Dr. H. W. KO for experimental work leading to the preliminary Kr/SiO₂ data.

* *Note added in proof:* Preliminary values for E and D_0 for Kr in fused SiO₂ (G. E. Type 151) are now available; they are 38.5 (kcal/mole) and 3.0×10^{-4} (cm²/sec), respectively (not corrected for grain size distribution).

²⁶ W. W. BRANDT, T. IKEDA, and Z. A. SCHELLY, to be published.

²⁷ W. H. ZACHARIASEN, J. Amer. Chem. Soc. **54**, 3841 [1932].